Journal of the Egyptian Mathematical Society (2013) **21**, 162–168

Egyptian Mathematical Society

Journal of the Egyptian Mathematical Society

www.etms-eg.org
www.elsevier.com/locate/joems

ORIGINAL ARTICLE

A novel statistical approach for detection of suspicious regions in digital mammogram

Z.A. Abo-Eleneen [a,b,*], **Gamil Abdel-Azim** [c]

[a] *College of Computer & Informatics, Zagazig University, Egypt*
[b] *College of Sciences, Qassim University, Saudi Arabia*
[c] *College of Computer & Informatics, Canal Suez University, Egypt*

Received 29 November 2012; revised 27 January 2013; accepted 1 February 2013
Available online 19 April 2013

KEYWORDS

Segmentation image;
Mammography images;
Breast cancer;
Fisher information measure;
Information theory

Abstract In this paper, we propose a novel algorithm to detect the suspicious regions on digital mammograms that based on the Fisher information measure. The proposed algorithm is tested different types and categories of mammograms (fatty, fatty-glandular and dense glandular) within mini-MIAS database (Mammogram Image Analysis Society database (UK)). The proposed method is compared with a different segmentation based information theoretical methods to demonstrate their effectiveness. The experimental results on mammography images showed the effectiveness in the detection of suspicious regions. This study can be a part of developing a computer-aided decision (CAD) system for early detection of breast cancer.

MATHEMATICS SUBJECT CLASSIFICATION: 60F05, 62F15, 62E20, 62G30

1. Introduction

Breast cancer is the most common malignancy in women and it has been proved that an early diagnosis of the disease can help strongly to enhance the expectancy of survival [1]. Understanding the nature of data and the information in mammography images is very important for developing a model that helps to diagnosis early the breast cancer. The presence of a breast mass is an alert sign, but it does not always indicate a malignant cancer. Fine needle aspiration (FNA) is an outpatient procedure that involves using a small-gauge needle to extract fluid directly from a breast mass [2]. But FNA of breast masses is a cost-effective.

In breast mammography images, bright regions represent cancer. In this paper, we propose a new method based on the Fisher information measurer to detect the bright regions (suspicion region) in the mammography images.

The Fisher Information measure (FIM) is an important concept in statistical estimation theory and information theory. To our knowledge; FIM have been not seen for the mammogram segmentation. The using of FIM for the segmentation

* Corresponding author at: College of Computer & Informatics, Zagazig University, Egypt.
E-mail addresses: Zaher_aboeleneen@yahoo.com (Z.A. Abo-Eleneen), gazim3@gmail.com, abdaladiem@qu.edu.sa (G. Abdel-Azim).

Peer review under responsibility of Egyptian Mathematical Society.

ELSEVIER Production and hosting by Elsevier

1110-256X © 2013 Production and hosting by Elsevier B.V. on behalf of Egyptian Mathematical Society. Open access under CC BY-NC-ND license.
http://dx.doi.org/10.1016/j.joems.2013.02.002

problem coming to formulate a novel objective function based on FIM. The proposed method determines threshold that is maximize the measure of separability of the resultant classes in gray levels.

Medical images are more sensitive as compared to ordinary images. Suspicious regions of medical images contain clinical information. Thus, correct segmentation of suspicious regions are very important to prevent false positive and false negative readings of mammogram. Suspicious regions are extracted from the background using a threshold value in the mammogram. Regions having gray levels below the threshold are assigned as background and regions having gray levels above the threshold are assigned as suspicious regions. Thus, suspicious regions correspond to the white regions in the output image. The mammogram image consists of three classes. The mammogram segmentation helps the specialists to find suspicious areas, and to separate the suspicious areas from the background [3]. The segmentation of mammogram is an essential and important step that determines the sensitivity of the computer aided decision (CAD) diagnoses system.

Thresholding methods can be classified into two groups, namely, global methods and local methods [4]. A global thresholding techniques are based on the global information, such as the gray level histogram of the image. Local threshold techniques partition the given image into a number of sub images and threshold value is determined locally. Main advantages of global thresholding are easy to implement and are computationally less involved. Many techniques of the global thresholding have been developed over the years to segment images [5–7]. Many segmentation techniques originated from the information theory such as Shannon entropy [8], Tsallis entropy, and its improvement [9,10]. The principle of entropy is to use uncertainty as a measure for describing the information that is contained in a source. Maximum information is achieved when no a prior knowledge is available, in which case the result is maximum uncertainty. These techniques have been used to segment the suspicion region in mammograms [11]. A quantity that is related to the Shannon entropy is the FIM [12]. This quantity has two basic roles to play in theory. First, it is a fundamental principle of the statistical field of study called parameter estimation. Second, it is a measure of the state of disorder of a system or phenomenon.

In this paper, we propose a new thresholding techniques based on FIM. It determines a suitable threshold values for segmentation mammogram, which helps to detect the suspicious regions. We apply the proposed method on several different kinds of standard test images (fatty, fatty glandular and dense-glandular) of mini-MIAS database (Mammogram Image Analysis Society database (UK)) to demonstrate their effectiveness and usefulness.

The rest of the paper is organized as follow: Section 2 describes the basic concepts of FIM and its implementation, with discussing the basic idea for segmentation of the suspicious regions of mammograms based on FIM. Section 3 discuses the experimental results and performance measure. Finally the conclusion presents in Section 4.

2. Fisher information measure and information theory

In this section, the FIM concept and Shannon entropy measure are reviewed. A new thresholding objective function for the mammogram images and the corresponding algorithm are then proposed.

2.1. Fisher information measure

The concept of the FIM was introduced by Fisher [13]. The FIM has a great utility in physics as well. FIM essentially describes the amount of information data provide about an unknown parameter. It has applications both in finding the variance of an estimator through the Cramer–Rao inequality and in the asymptotic behavior of maximum likelihood estimates [13]. Let X be a random variable, and let $p(x;\theta)$ be the probability density (mass) function for some model of the data that have the parameter θ. The FIM is given by the following [13].

$$I(\theta) = -E\left(\frac{d^2 \log p(x;\theta)}{d\theta^2}\right) = E\left(\frac{d \log p(x;\theta)}{d\theta}\right)^2. \quad (1)$$

The special case of translation families deserve special mention. These are mono parametric families of distribution of the form $p(x-\theta)$ which are known up to the shift parameter θ All members of the family possess identical shape, and here FIM adopts the appearance

$$I(X) = \int \left(\frac{d \log p(x)}{dx}\right)^2 p(x)dx = -\int \frac{d^2 \log p(x)}{dx^2} p dx. \quad (2)$$

This form of Fisher information measure constitute the main ingredient of a powerful variational principal devised by Frieden [12], that gives rise to a substantial portion of the physics. In the consideration, that follow we shall restrict ourselves to the form (2) of FIM.

2.2. Fisher information measure vs. entropy

Let X be a physical system that takes on a finite or accountably infinite number N of values that are characterized by the probability density p_i, $i \in \mathrm{N}$ where p_i is the probability of x_i and $x_i \in (a,b) \subseteq \Re$, is assumed to be normalized to unity so that $\sum_{i=1}^{N} p_i = 1$. In this case, X can be specified by a probability vector, $P = \{p_1, p_2, \ldots, p_N\}$. Its distribution over the interval (a, b) can be studied by using the following complementary spreading and information-theoretic measures: the FI measure [12,15] and the Shannon entropy [14].

The principle of maximal entropy (Boltzmann) is frequently used to indicate the amount of information produced in a certain source, and is also used to measure the disorder or complexity of a dataset and defined by [14]

$$H(X) = -\sum_i p(x_i) \log p(x_i). \quad (3)$$

A second measure of disorder, beside entropy, exists which is called Fisher information. The FIM [12,16] of X are defined by the following.

$$I(X) = \sum_i \frac{(p(x_{i+1}) - p(x_i))^2}{p(x_i)}, \quad (4)$$

which follows from a suitable discretization of (2). In analogy to Eq. (3) for the entropy H. The most obvious difference between (2) and (3) is the fact that (2) contains a derivative while (3) does not. As a consequence, extremizing these two functionals yields fundamentally different equations for the

probability function P, namely a differential equation for the Fisher functional I and an algebraic equation for the entropy functional H. Thus, whereas Shannon entropy is a global measure of smoothness in $p(x)$, FIM is a local measure. Hence, when extremized through the variation of $p(x)$, Fisher's form gives a differential equation whereas Shannon's form always gives directly the same form of solution, an exponential function [12]. Therefore, if one of the two measures Shannon entropy (global) or FIM (local) is to be used in a variation principle in order to derive the physical law $p(x)$ describing a general scenario, a preference is given to the local measure, FIM [12,16]. For different applications of FIM and more comparisons among the FIM and information-theoretic measures we refer the reader to the book by Frieden [12].

2.3. Fisher information and information theory mammogram thresholding

Mammogram consists of three objects namely breast background, tissue background and suspicious region. Breast background does not provide any information in diagnosis. So, breast background can be ignored in mammogram analysis study. Approximately, more than one-third of a mammogram is breast background. It could affect the average gray level value of the breast tissues. Hence, the average gray level value of the breast tissues is defined as follows by excluding breast background pixels [17,18]

$$k = \frac{1}{n}\sum_{i,j\in R}^{MN} f(i,j). \tag{5}$$

where M and N are dimensions of the mammogram, R is the region having gray level values greater than 100, n is the number of pixels in this region and $f(i, j)$ is the gray level value at the coordinates i and j. Let I denote a gray-scale image with L gray levels $[0, 1, \ldots, L]$. The number of pixels with gray level i is denoted by n_i and the total number of pixels by $N = n_0 + n_1 + \cdots + n_L$. The probability of gray level i appeared in the image is defined as:

$$p_i = \frac{n_i}{N}, \quad p_i \geqslant 0, \quad \sum_{i=0}^{L} p_i = 1.$$

Suppose that the pixels in the image are divided into three classes A, B and C by a gray level t; A is the set of pixels with levels $[0, 1, \ldots, k]$, B is the set of pixels with levels $[k + 1, k + 2, \ldots, t]$ and the rest of pixels belongs to C; where, A, B and C are normally correspond to the breast background, tissue background and suspicious region respectively. We can derive three probability distributions, one for the breast background, second for the tissue background and third for the suspicious region is shown as the following: probability distribution of breast background:

$$P_A = \frac{p_1}{w_1}, \frac{p_2}{w_1}, \ldots, \frac{p_k}{w_1},$$

the probability distribution of tissue background:

$$P_B = \frac{p_{k+1}}{w_2 - w_1}, \frac{p_{k+2}}{w_2 - w_1}, \ldots, \frac{p_t}{w_2 - w_1},$$

and the probability distribution of suspicious region:

$$P_C = \frac{p_{t+1}}{1 - w_2}, \frac{p_{t+2}}{1 - w_2}, \ldots, \frac{p_L}{1 - w_2},$$

where

$$w_1 = \sum_{i=1}^{k} p_i, \quad w_2 = \sum_{j=1}^{t} p_j,$$

and t is the threshold value. Then the Shannon entropy [4] based thresholding selected a threshold t^* maximizing the criterion

$$t^* = \max_t [S_B(t) + S_C(t)], \tag{6}$$

where

$$S_B(t) = \frac{1}{w_2 - w_1}\sum_{i=k+1}^{t} p(x_i)\log(p(x_i)),$$

and

$$S_C(t) = \frac{1}{1 - w_2}\sum_{i=t+1}^{L} p(x_i)\log(p(x_i)).$$

The Reny entropy [19] based thresholding selected a threshold t^* maximizing the criterion

$$t^* = \max_t [R_B(t) + R_C(t)], \tag{7}$$

where

$$R_B(t) = \frac{1}{(1-\alpha)}\log_e\left[\sum_{i=k+1}^{t}\left(\frac{p(x_i)}{(w_2 - w_1)}\right)^{\alpha}\right],$$

$$R_C(t) = \frac{1}{(1-\alpha)}\log_e\left[\sum_{i=t+1}^{L}\left(\frac{p(x_i)}{(1 - w_2)}\right)^{\alpha}\right], \quad \text{and } \alpha \neq 1,\ \alpha \succ 0.$$

The Kapur entropy based thresholding [4] selected a threshold t^* maximizing the criterion

$$t^* = \max_t [K_B(t) + K_C(t)], \tag{8}$$

where

$$K_B(t) = \frac{1}{(\beta-\alpha)}\log_e\left[\sum_{i=k+1}^{t}\frac{\left(\frac{p(x_i)}{w_2 - w_1}\right)^{\alpha}}{\left(\frac{p(x_i)}{1 - w_2}\right)^{\beta}}\right],$$

$$K_C(t) = \frac{1}{(\beta-\alpha)}\log_e\left[\sum_{i=t+1}^{L}\frac{\left(\frac{p(x_i)}{w_2 - w_1}\right)^{\alpha}}{\left(\frac{p(x_i)}{1 - w_2}\right)^{\beta}}\right], \quad \text{and } \alpha \neq \beta,\ \alpha \succ 0,\ \beta \succ 0.$$

Finally Harvrda and Charvat entropy based thresholding [10] selected a threshold t^* maximizing the criterion

$$t^* = \max_t [HC_B(t) + HC_C(t) + (1-\alpha)(HC_B(t) + HC_C(t))], \tag{9}$$

where

$$HC_B(t) = \frac{1}{(1-\alpha)}\left[\sum_{i=k+1}^{t}\left(\frac{p(x_i)}{(w_2 - w_1)}\right)^{\alpha} - 1\right],$$

and

$$HC_C(t) = \frac{1}{(1-\alpha)}\left[\sum_{i=t+1}^{L}\left(\frac{p(x_i)}{(1 - w_2)}\right)^{\alpha} - 1\right], \quad \text{and } \alpha \neq 1,\ \alpha \succ 0.$$

The new method proposes an optimality criterion based on the FIM. Based on the definition of FIM in Eq. (4), the priori FIM

of tissue background pixels and the FIM of the suspicious region pixels can be defined as follows respectively:

$$FIM_B(t) = \frac{1}{w_2 - w_1} \sum_{i=k+1}^{t} \frac{(p(x_{i+1}) - p(x_i))^2}{p(x_i)},$$

$$FIM_C(t) = \frac{1}{1 - w_2} \sum_{i=t+1}^{L} \frac{(p(x_{i+1}) - p(x_i))^2}{p(x_i)}.$$

The FIM is parametrically dependent upon the threshold value t for the foreground and background. We define the FIM within the two classes as the following

$$FIM(t) = (w_2 - w_1)FIM_B(t) + (1 - w_2)FIM_C(t).$$

We maximize the information measure within the two classes (the suspicious region and the tissue background). When $FIM(t)$ is maximized, the luminance level t is considered to be the optimum threshold value

$$t_{opt} = \arg \max[FIM(t)]. \quad (10)$$

2.4. Algorithm

The following steps describe the proposed algorithm for image segmentation:

1. Let max = 0 be the optimal threshold, and let max *FIM* be the maximum value of the objective function.
2. For $t = 1$ to Maximum of gray intensities
3. Compute the function objective value that corresponds to the gray level t

If $FIM(t) >$ max, Then max = $FIM(t)$, Topt = t. End.
Take Topt as the optimal threshold for segmenting the image.

3. Experimental results and discussion

Experiments are conducted on images of mini-MIAS database (Mammogram Image Analysis Society database (UK)), to demonstrate the effectiveness and usefulness of the proposed method. Several different kinds of standard test images (fatty, fatty-glandular and dense glandular) of mini-MIAS database are segmented. We pick randomly more than one mammogram of each kind. The results yield by the proposed method compared with the most commonly information theoretic methods used in literature. Namely Shannon entropy, Renyi entropy, Havrda & Charvat and Kapur entropy described by Eqs. (6)–(9). The mammograms with their gray level histograms and the segmented images obtained by using the proposed method, that based on FIM are displayed in Figs. 1.1, 2.1 and 3.1; while The results yield by Renyi entropy, Havrda & Charvat and Kapur entropy methods are displayed in Figs. 1.2, 2.2 and 3.2. In order to objectively assess the proposed method, the uniformity measure, is used for performance evaluation.

The quality of the results is compared quantitatively by using the uniformity measure besides the visual perception. From Figs. 1.1, 2.1 and 3.1, it can easily observe that the suspicion region based on the proposed method is well segmented. In order to avoid human interpretation, we use the measure of uniformity [20,21], for performance evaluation.

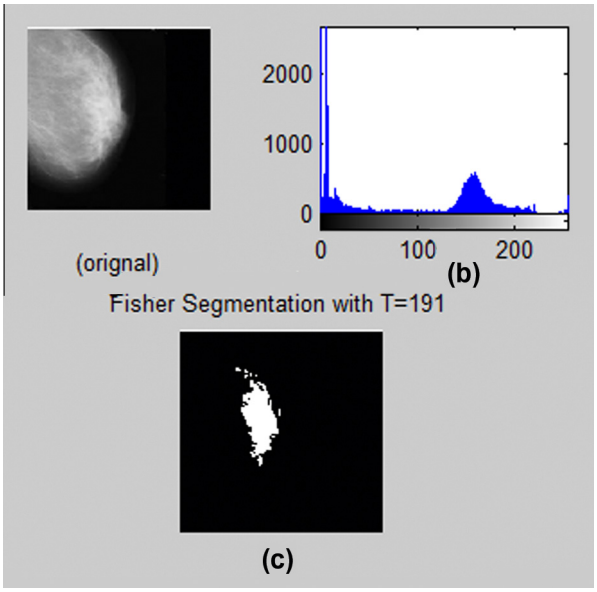

Figure 1.1 (a) Fatty-glandular mammogram (mdb218) of mini-MIAS database, (b) its gray level histogram, and (c) segmented image using FIM.

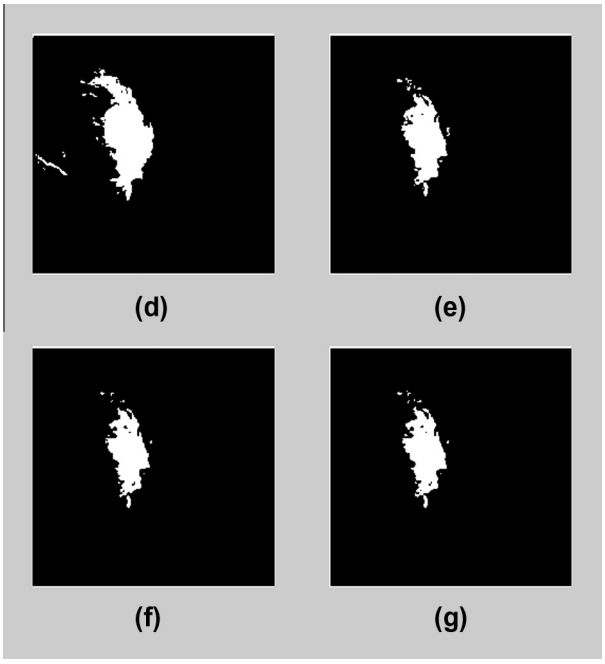

Figure 1.2 (d) Shannon entropy threshold $t = 180$, (e) Renyi entropy threshold $t = 191$ with $\alpha = 0.7$, (f) Havrda & Charvat entropy threshold $t = 194$ with $\alpha = 0.2$, and (g) Kapur entropy threshold $t = 191$.

The uniformity measure is generally used to describe region homogeneity in an image. For a given threshold t, it is defined by

$$U(t) = 1 - \frac{\sigma_B^2(t) + \sigma_F^2(t)}{C}, \quad (11)$$

where B and F represent background and foreground regions, $f(x, y)$ is the grey level of the pixel (x, y)

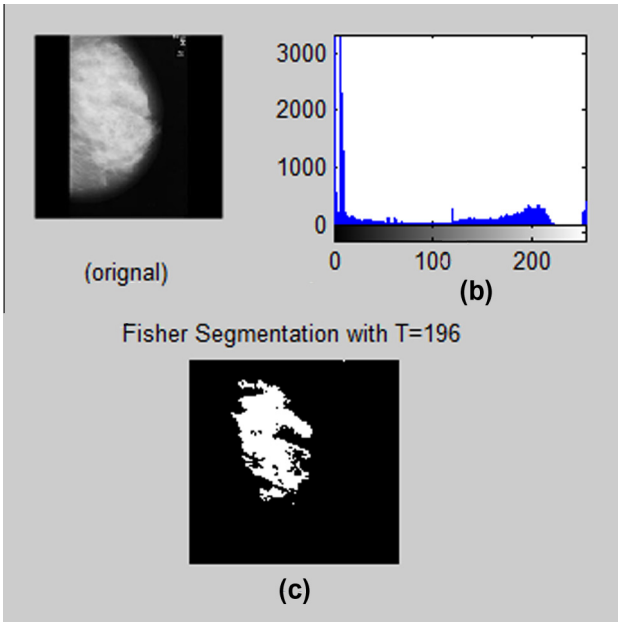

Figure 2.1 (a) Dense-glandular mammogram (mdb236) of mini-MIAS database, (b) its gray level histogram, and (c) segmented image using FIM.

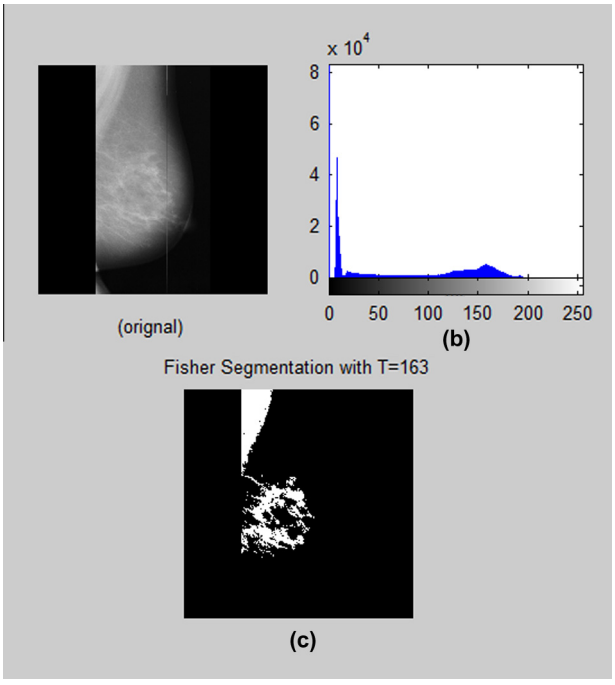

Figure 3.1 (a) Fatty mammogram (mdb238) of mini-MIAS database, (b) its gray level histogram, and (c) segmented image using FIM.

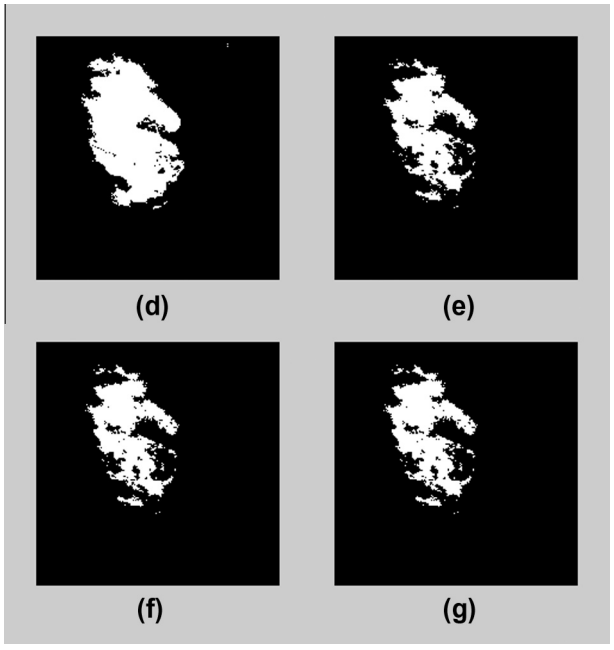

Figure 2.2 (d) Shannon entropy threshold $t = 186$, (e) Renyi entropy threshold $t = 200$ with $\alpha = 0.7$, (f) Havrda & Charvat entropy threshold $t = 201$ with $\alpha = 0.2$, and (g) Kapur entropy threshold $t = 201$ with $\alpha = 0.5$, $\beta = 0.7$.

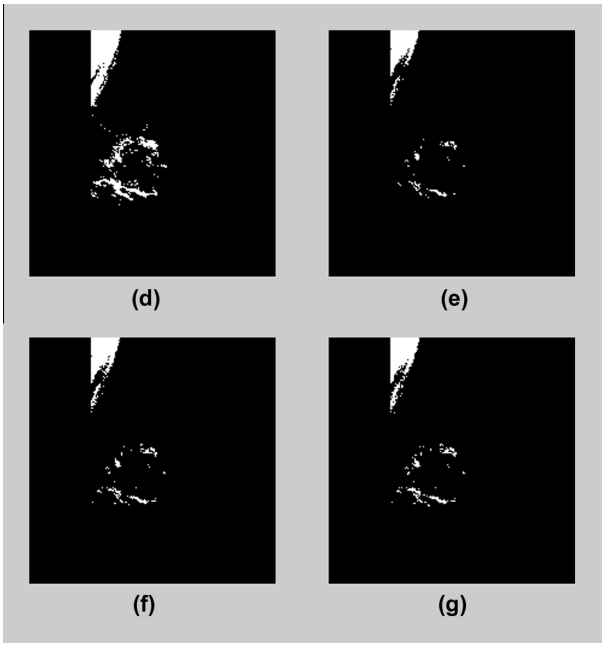

Figure 3.2 (d) Shannon entropy threshold $t = 171$, (e) Renyi entropy threshold $t = 179$ with $\alpha = 0.7$, (f) Havrda & Charvat entropy threshold $t = 178$ with $\alpha = 0.2$, and (g) Kapur entropy threshold $t = 177$ with $\alpha = 0.5$, $\beta = 0.7$.

Table 1 The threshold values for Shannon, Renyi with $\alpha = 0.7$, Havrda & Charvat with $\alpha = 0.2$, Kapur with $\alpha = 0.5$, $\beta = 0.7$ and the proposed method. With the measure of uniformity $U(t)$.

	mdb218		mdb236		mdb238		mdb219		mdb222	
	t	$U(t)$	t	$U(t)$	t	$U(t)$	t	$U(t)$	t	$U(t)$
Shannon	180	8.56E−01	186	8.95E−01	171	8.51E−01	185	8.46E−01	186	8.38E−01
Renyi with $\alpha = 0.7$	191	8.47E−01	200	8.54E−01	179	8.36E−01	194	8.40E−01	193	8.23E−01
Havrda with α 0.2,	194	8.45E−01	201	8.50E−01	178	8.37E−01	198	8.38E−01	194	8.21E−01
Kapur $\alpha = 0.5$, $\beta = 0.7$	193	8.46E−01	201	8.50E−01	177	8.40E−01	198	8.38E−01	194	8.21E−01
ProposedMethod	191	8.47E−01	196	8.68E−01	178	8.37E−01	189	8.43E−01	193	8.23E−01

Table 2 The threshold values for Shannon, Renyi with $\alpha = 0.7$, Havrda & Charvat with $\alpha = 0.2$, Kapur with $\alpha = 0.5$, $\beta = 0.7$ and the proposed method. With the measure of uniformity $U(t)$.

	mdb227		mdb240		mdb245		mdb248		mdb253	
	t	$U(t)$	t	$U(t)$	t	$U(t)$	t	$U(t)$	t	$U(t)$
Shannon	184	8.56E−01	198	8.29E−01	177	8.83E−01	177	8.61E−01	191	8.69E−01
Renyi with $\alpha = 0.7$	193	8.39E−01	210	7.77E−01	198	8.70E−01	192	8.51E−01	203	8.10E−01
Havrda with α 0.2,	194	8.37E−01	210	7.77E−01	200	8.69E−01	193	8.51E−01	205	7.96E−01
Kapur $\alpha = 0.5$, $\beta = 0.7$	194	8.37E−01	210	7.77E−01	199	8.70E−01	194	8.52E−01	205	7.96E−01
ProposedMethod	195	8.36E−01	218	7.48E−01	192	8.73E−01	184	8.55E−01	207	7.82E−01

$$C = \frac{1}{2}(f_{\max} - f_{\min})^2, \quad \mu_B^t = \frac{\sum_{(x,y)\in B} f(x,y)}{n_B^t},$$

$$\mu_F^t = \frac{\sum_{(x,y)\in F} f(x,y)}{n_F^t},$$

$$\sigma_B^2(t) = \frac{1}{n_F^t} \sum_{(x,y)\in B} (f(x,y) - \mu_B)^2,$$

$$\sigma_F^2(t) = \frac{1}{n_F^t} \sum_{(x,y)\in F} (f(x,y) - \mu_F)^2,$$

n_B^t is the number of pixels in background region and n_F^t is the number of pixels in foreground region. Maximising $U(t)$ [20] is equivalent to minimising Var^t within-classes, which is also equivalent to maximizing Var^t between-classes and the threshold value produced by Otsu's method, t is identical to the t that maximises $U(t)$ in [21]. It should be noted that the values of $U(t)$ vary with images. However, the normalization constant C in $U(t)$ is independent of the threshold value t. In this case, C can be chosen to normalise the values of $U(t)$ to the range of [0, 1] such that the minimum and maximum of $U(t)$ for each image were always set to 0 and 1 respectively for comparison. Using this process, the uniformity values calculated from $U(t)$ in the following experiments are always in between 0 and 1.

Tables 1 and 2 show that the proposed method gives good results of segmentation according to the values of $U(t)$

4. Conclusion and future works

Fisher information is a measure of the state of disorder of a system or phenomenon; thus, it plays an important role in terms of physical theory. In this paper, we have developed a simple but effective method of digital mammograms segmentation that employs the FIM. The underlying idea of the proposed method is to maximize the FIM of the object and background classes. The application has been taken on a several different kinds of mammogram images (fatty, fatty-glandular and dense-glandular) of mini-MIAS database.

The study shows that the results of FIM to separate suspicious region from the tissue background in mammogram images are well segmented. The detection of suspicious region is quite promising. The proposed method can be very useful for radiologists to find suspicious region in mammogram. Thus, it will be useful to control the breast cancer. In future work, various effective features will be extracted from suspicious region of mammogram to characterize suspicious region as benign or malignant. This study can be a part of developing a computer aided decision (CAD) system for early detection of breast cancer.

Acknowledgement

The authors would like to express deep thanks to the two referees for their helpful comments and suggestions which led to a considerable improvement in the presentation of this paper.

References

[1] C. Venanzi, A. Bergamaschi, F. Bruni, D. Dreossi, R. Longo, A. Olivo, S. Pani, E. Castelli, A digital detector for breast computed tomography at the SYRMEP beam line, Nuclear Instruments and Methods in Physics Research Section A: Accelerators, Spectrometers, Detectors and Associated Equipment 548 (2005) 264–268.

[2] O.L. Mangasarian, W.N. Street, W.H. Wolberg, Breast cancer diagnosis and prognosis via linear programming. Mathematical Programming Technical Report 94-10, University of Wisconsin, 1994.

[3] Abou Ella Hassanien, Fuzzy rough sets hybrid scheme for breast cancer detection, Journal of Image and Vision Computing 25 (2007) 172–183.

[4] P.K. Sahoo, S. Soltani, A.K.C. Wong, Y.C. Chen, A survey of the thresholding, Journal of Computer Vision Graphic Image Processing 41 (1998) 233–260.
[5] C.H. Li, C.K. Lee, Minimum cross entropy thresholding, Journal of Pattern Recognition 26 (1993) 617–625.
[6] R. Nikhil Pal, On minimum cross entropy thresholding, Journal of Pattern Recognition 29 (1996) 575–580.
[7] L. Paul Rosin, Unimodal thresholding, Journal of Pattern Recognition 34 (2001) 2083–2096.
[8] C.E. Shannon, A mathematical theory of communication, International Journal of Bell System Technical 27 (1948) 379–423.
[9] M. Portes de Albuquerque, I.A. Esquef, A.R. Gesualdi, Mello, image thresholding using tsallis entropy, Journal of Pattern Recognition Letters 25 (2004) 1059–1065.
[10] K. Prasanna, P.K. Sahoo, Gurdial Arora, Image thresholding using: two-dimensional Tsallis–Havrda–Charvat entropy, Journal of Pattern Recognition Letters 27 (2006) 520–528.
[11] Baljit Singh Khehra, in: Proceedings of the World Congress on Engineering II WCE, July 6–8, London, UK, 2011.
[12] B.R. Frieden, Science from Fisher Information: A Unification, Cambridge University Press, Cambridge, UK, 2004.
[13] R.A. Fisher, Theory of statistical estimation, Proceedings of the Cambridge Philosophical Society 22 (1925) 700–725.
[14] B.R. Frieden, Fisher information, disorder, and the equilibrium distribution of physics, Physical Review A 41 (1990) 4265–4276.
[15] T.M. Cover, J.A. Thomas, Elements of Information Theory, Wiley, N.Y., 1991.
[16] J.S. Dehesa, R.J. Yanezz, R. Alvarez-Nodarsex, P. S_anchez-Morenoy, Information-theoretic measures of discrete orthogonal polynomials, Journal of Difference Equations and Applications 15 (2004) 1–17.
[17] H.D. Cheng, Y.M. Lui, R.I. Freimanis, A novel approach to micro calcification detection using fuzzy logic technique, IEEE Transactions on Medical Imaging 17 (1998) 442–450.
[18] Mohanalin, Prem Kumar Kalra, Nirmal Kumar, An automatic method to enhance micro calcifications using normalized Tsallis entropy, Journal of Signal Processing 90 (2010) 952–958.
[19] Wang Shitong, F.L. Chung, Note on the equivalence relationship between Renyi-entropy based and Tsallis-entropy based image thresholding, Journal of Pattern Recognition Letters 26 (2005) 2309–2312.
[20] S.U. Lee, S.Y. Chung, R.H. Park, A comparative performance study of several global thresholding techniques for segmentation, Computer Vision, Graphics, and Image Processing 52 (1990) 171–190.
[21] C.I. Chang, Y. Du, J. Wang, S.M. Guo, P.D. Thouin, Survey and comparative analysis of entropy and relative entropy thresholding techniques, IEE Proceedings – Vision, Image and Signal Processing 153 (2006) 837–850.